Laboratory Investigation (2020) 100:1551–1563
https://doi.org/10.1038/s41374-020-0462-z

ARTICLE

PCP4/PEP19 downregulates neurite outgrowth via transcriptional regulation of Ascl1 and NeuroD1 expression in human neuroblastoma M17 cells

Ikumi Kitazono[1] · Taiji Hamada[1] · Takuya Yoshimura[2] · Mari Kirishima[1] · Seiya Yokoyama[1] · Toshiaki Akahane[1] · Akihide Tanimoto[1]

Received: 19 January 2020 / Revised: 5 June 2020 / Accepted: 22 June 2020 / Published online: 8 July 2020
© The Author(s), under exclusive licence to United States and Canadian Academy of Pathology 2020

Abstract

Purkinje cell protein 4/peptide 19 (PCP4/PEP19) is 7.6 kDa peptide originally found in Purkinje cells. PCP4/PEP19 is a differentiation maker of Purkinje cells, where it functions as an antiapoptotic factor. Cerebral neuronal cells also express PCP4/PEP19, which may be related to neuronal cell survival. However, evidence suggests that PCP4/PEP19 may also be involved in neuronal differentiation. Here, we investigated the effects of PCP4/PEP19 expression on neuronal differentiation by analyzing neurite outgrowth, and expression of neuronal differentiation markers in cultured human neuroblastoma M17 cells. When PCP4/PEP19 expression was reduced by siRNA-mediated knockdown, neurite outgrowth was significantly increased. Among many differentiation markers tested, expression of NeuroD1 was increased, while that of Ascl1 was decreased upon PCP4/PEP19 knockdown. Furthermore, luciferase reporter assays revealed that PCP4/PEP19 knockdown upregulated NeuroD1 and downregulated Ascl1 expression, at the transcriptional level. These results suggest a new function of PCP4/PEP19, which suppresses neurite outgrowth and neuronal differentiation through the regulation of NeuroD1 and Ascl1 expression in M17 cells. Furthermore, immunohistochemical studies showed that PCP4/PEP19 localizes in the nuclei of human neuroblastoma cells. Therefore, PCP4/PEP19 may also be an intranuclear negative regulator of neuronal differentiation and may thus be a potential therapeutic target to promote cellular differentiation in human neuroblastoma.

Introduction

Purkinje cell protein 4/peptide 19 (PCP4/PEP19) is expressed in the Purkinje cells and stellate neurons in the cerebellum [1]. PCP4/PEP19 was first identified in the rat cerebellar extracts as a developmentally regulated polypeptide of 7.6 kDa that possess regions homologous to the calcium-binding β-chain of S100 protein [2]. PCP4/PEP19 is a calmodulin (CaM)-binding protein and regulates CaM-dependent signaling, which controls various neuronal processes and functions. In fact, PCP4/PEP19-null mice exhibit impaired learning of locomotor tasks and autonomic function [3]. In addition, mice overexpressing PCP4/PEP19 as a model for Down syndrome show precocious neural differentiation and learning impairment [4]. In human, neural expression of PCP4/PE19 decreases in Alzheimer's and Huntington's disease, as well as with alcoholism [5, 6]. Therefore, evidence indicates that PCP4/PEP19 is essential for the central nervous development and differentiation, and for higher brain functions.

PCP4/PEP19 is expressed in some human tumor cells, including breast cancer, adrenal cortical adenoma, and uterine leiomyoma [7–10]. In our previous studies, we showed that PCP4/PEP19 inhibits cancer cell apoptosis and enhances the migratory and invasive phenotypes, thus regulating the epithelial–mesenchymal transition. It also induces aromatase expression for paracrine estrogen supply in human breast cancer cells [8, 11, 12]. These findings suggest that PCP4/PEP19 may be a potential molecular target to suppress cancer cell proliferation, invasion, and metastasis.

Rat chromaffin PC12 cells are derived from pheochromocytoma cells and share common features with postganglionary

✉ Akihide Tanimoto
akit09@m3.kufm.kagoshima-u.ac.jp

[1] Department of Pathology, Kagoshima University Graduate School of Medical and Dental Sciences, Kagoshima, Japan

[2] Department of Oral and Maxillofacial Surgery, Kagoshima University Graduate School of Medical and Dental Sciences, Kagoshima, Japan

sympathetic neurons as paraneurons. Therefore, PC12 cells are commonly used to study neuronal cell death and differentiation. In PC12 cells, PCP4/PEP19 expression promotes neuroendocrine differentiation and neurotransmitter release [13], and regulates the apoptotic cell death [14].

In this study, we examined the effects of PCP4/PEP19 expression on neuronal differentiation using cultured M17 cells (BE(2)-M17 cells, a clone of the SK-N-BE(2) human neuroblastoma cell line). This poorly differentiated neuroblastoma-derived cell line is another model often used for functional and morphological studies of neurons, especially to study amyloid-β precursor protein processing [15]. Neurite outgrowth and expression of neuronal differentiation markers were quantified in M17 cells transfected with PCP4/PEP19 siRNA or treated with all-trans-retinoic acid (AtRA), a representative agent for neuronal differentiation [16]. In addition to its anti-apoptotic, antimigratory, and anti-invasive activities [8, 11, 12], our findings suggest that PCP4/PEP19 could also have an inhibitory effect on cellular differentiation, at least in human-derived neuroblastoma cell line in culture. Therefore, PCP4/PEP19 may be a molecular target to induce differentiation of neuroblastoma cells, which would be another treatment strategy for cancers with poorly differentiated and highly aggressive cells.

Materials and methods

Cells and cell culture

Human neuroblastoma M17 and SH-SY5Y cells, and human breast cancer SK-BR-3 cells were obtained from American Type Culture Collection (Rockville, MD, USA). Cells were maintained in a 1:1 mixture of minimal essential medium (MEM, Sigma-Aldrich, St. Louis, MO, USA) and F12 medium (Nissui, Tokyo, Japan) for M17 and SH-SY5Y cells, and McCoy's 5A (Thermo Scientific, Waltham, MA, USA) for SK-BR-3 cells, supplemented with 2 mM glutamine, 100 U/mL penicillin, 100 µg/mL streptomycin (Thermo Fisher Scientific), and 10% fetal bovine serum (FBS, Sigma-Aldrich, St Louis, MS, USA) at 37 °C with 95% air and 5% CO_2. For cellular differentiation, M17 cells were given differentiation medium every 2 days (MEM/F12 containing 2% FBS) with 10 µM AtRA (FUJIFILM Wako Pure Chemical, Osaka, Japan).

Transfection experiments

M17 cells were subcultured in appropriate plates or dishes for experiments, and transfected the next day with predesigned siRNA (ID: HSS143251) for knockdown of PCP4/PEP19 or Stealth RNAi siRNA Negative Control (Thermo Fisher Scientific) using ScreenFect siRNA (FUJIFILM Wako Pure Chemical). For PCP4/PEP19 overexpression experiments in SH-SY5Y cells, a CMV-driven expression vector harboring PCP4/PEP19 cDNA (OriGene Technologies, Rockville, MD, USA) was transfected using Lipofectamine 3000 (Thermo Fisher Scientific). After 5 days of AtRA treatment, the cells were harvested and extracted mRNA was subjected to qRT-PCR for the detection of PCP4/PEP19, Ascl1 and NeuroD1 mRNA expression.

Cell proliferation assay

M17 cells were seeded at 1×10^4 cells/well in 96-well plates in the medium supplemented with 10% FBS, and allowed to adhere overnight. The cells were transfected with either PCP4/PEP19 or control siRNAs, and the transfection medium was replaced with differentiation medium containing 10 µM AtRA on the next day. Then the cells were incubated to assay cell proliferation for 5 days. Cell Counting Kit-8 (WST-8, Dojindo, Kumamoto, Japan) was used for viable cell counting at the indicated time.

Expression and purification of Tag fusion PCP4/PEP19

Trigger factor (TF)- or GST-tagged PCP4/PEP19 expression plasmid was transfected into *E. coli* DH5α (Toyobo, Osaka, Japan), and the bacterial cells were cultured in LB medium (Becton Dickinson, Franklin Lakes, NJ, USA) with 100 µg/mL ampicillin. At optical density (600 nm) of 0.2–0.3, PCP4/PEP19 expression was induced with 0.1 or 0.5 mM isopropyl-β-D-thiogalactopyranoside (FUJIFILM Wako Pure Chemical) for 20 h at 25 or 15 °C. The bacterial pellet was resuspended in PBS, lysed using lysis buffer (1 mM EDTA, 1% Triton X-100, 1 mM DTT, 1 mM PMSF, and 10 µg/mL leupeptin in PBS) by sonication on ice and the lysate was cleared by 60 min centrifugation at 20,000 × *g* at 4 °C. TF-tagged PCP4/PEP19 was purified using a Ni Sepharose 6 Fast Flow affinity column (His GraviTrap, GE Healthcare, Chicago, IL, USA). GST-tagged PCP4/PEP19 was purified using a Glutathione Sepharose 4B affinity column (GST GraviTrap, GE Healthcare).

Antibody production and purification

For the first immunization, purified TF-tagged PCP4/PEP19 in PBS was mixed with an equal volume of Freund's complete adjuvant. Guinea pigs were injected subcutaneously at several different sites. Five booster injections were given with the PCP4/PEP19 mixed with incomplete Freund's adjuvant at 2-week intervals. Whole blood was drawn 10 days after the last injection. Polyclonal antibodies against PCP4/PEP19

were purified from serum by affinity chromatography on GST-tagged PCP4/PEP19 or TF protein-coupled sepharose columns (HiTrap NHS-activated HP Columns, GE Healthcare).

Immunofluorescence

M17 cells were plated at a density of 5×10^3 cells in Permanox Plastic Chamber Slide (Thermo Fisher Scientific). After 5 days of siRNA transfection or AtRA treatment, cells were fixed with 4% paraformaldehyde (PFA) for 15 min at room temperature (RT), rinsed with PBS, and incubated in blocking solution (3% bovine serum albumin [BSA], 0.3% Triton X-100 in PBS) for 60 min at RT. Cells were then incubated at 4 °C with primary antibodies anti-β III tubulin (TU-20, 1:1000, Abcam, Cambridge, UK) prepared in dilution buffer (1% BSA, 0.3% Triton X-100 in PBS). After washing in PBS, the cells were incubated with secondary anti-mouse antibodies conjugated with Alexa Fluor 594 (Thermo Fisher Scientific) at a 1:1000 dilution for 1 h at RT. After washing in PBS, the coverslips were mounted with ProLong Diamond Antifade mounting medium (Thermo Fisher Scientific) with DAPI. For F-actin staining, cells were incubated with green fluorescent dye-labeled phalloidin (Acti-stain 488 Fluorescent Phalloidin, Cytoskeleton Inc., Denver, CO, USA) for 30 min before mounting the coverslip. Images were acquired using a fluorescence microscope (BX51, Olympus, Tokyo, Japan).

Neurite length measurement

After 5 day-AtRA treatment, M17 cells were fixed with 4% PFA, and neurites were visualized by immunofluorescence using anti-β III tubulin antibody. The images were randomly captured with fluorescence microscope (BX51, Olympus). The cell fluorescent image views with an appropriate cellularity to include cells with no overlapping each other were selected, and neurite outgrowth was morphologically evaluated. A length from the tip to root of neurites: neurite length was measured using the cellSens software (Olympus), and then numbers of neurites per cell and the numbers of cells with neurites were calculated in total of 30 cells.

Quantitative RT-PCR analysis for mRNA expression

Total RNA was extracted using ReliaPrep RNA Cell Miniprep System (Promega, Madison, WI, USA) and was converted into cDNA using a ReverTra Ace qPCR RT Master Mix (Toyobo). The cDNA was amplified by LightCycler 480 (Roche Diagnostics, Basel, Switzerland) using THUNDERBIRD Probe qPCR Mix and KOD SYBR qPCR Mix (Toyobo). Each sample was analyzed in triplicate in separate wells for the target and reference genes using the primers listed in Table 1 [17–20]. The average of three threshold cycle values for the target and reference genes was calculated and analyzed using the comparative Ct method.

Table 1 Primers for RT-qPCR in this study.

Target genes	Primer sequence (5′ – 3′)	References
PCP4/PEP19	Assay ID: Hs01113638_m1	Thermo Fisher Scientific
GAPDH	Assay ID: Hs99999905_m1	
HES1	CATTCCAAGCTGGAGAAGG and CTCGGTATTAACGCCCTCG	[28]
NOTCH1	CGGCCAGCAGATGATCTTCCC and CACACACTGCCGGTTGTCAATC	[28]
SOX2	CCACCTACAGCATGTCCTACTCG and GGGAGGAAGAGGTAACCACAGG	[29]
VIM	GGACCAGCTAACCAACGACAAA and CGCATTGTCAACATCCTGTCTG	[29]
ASCL1	GGAGCTTCTCGACTTCACCAAC and CAACGCCACTGACAAGAAAGC	[28]
NEUROD1	GAGACTATCACTGCTCAGGAC and CCTGAGAACTGAGACACTCGTC	[28]
DCX	AAGCTTAGGTGCCTGCGTTA and AAGGGGCACTTGTGTTTGTC	[28]
MAP2	AATAGACCTAAGCCATGTGACATCC and AGAACCAACTTTAGCTTGGGCC	[28]
TUBB3	GGCCAAGTTCTGGGAAGTCAT and CTCGAGGCACGTACTTGTGA	[29]
PCP2	GCCAGATCCAGCATCGTTGT and ACGTGGCTCAGCAGATTGAA	–
ID1	GGTAAACGTGCTGCTCTACGAC and GTCCCTGATGTAGTCGATGAC	[28]
ID3	CAGGTGGAAATCCTACAGCG and CGTTGGAGATGACAAGTTCCG	[28]
ETV1	CCCAGTGTATGAACACAACACC and TGGCTCTTGTTTGATGTCTCC	[30]
ETS1	ACATCATCCACAAGACAGCGG and CACACACAAAGCGGTACACGT	[31]
ETS2	GCTCCACGTTCTTCTGTGTGATT and CGTCCTTCAGCTCTGTACAGTAACT	[31]
GAPDH	CTGACTTCAACAGCGACACC and TAGCCAAATTCGTTGTCATACC	[28]

Plasmid construction for luciferase reporter assay and PCP4/PEP19 expression

Regulatory regions of human Ascl1 (−2086/+69) and NeuroD1 (−2101/+91) genes were generated from genomic DNA of M17 cells by PCR, using KOD FX Neo polymerase (Toyobo). The sequences of forward and reverse primers to amplify Ascl1 and NeuroD1 promoters were 5′-TAAACGCGTCTGGGTCATGTGGGAGGTGG GTA-3′ and 5′-TCAGCTCGAGTCCTTCTTTCACTCG CCCTCCCT-3′ (Ascl1); 5′-TACGGTACCCTGCGGCA GTAGTGTGCTGCCAGT-3′ and 5′-TGAAAGATCTGAA TTCCTCGTGTCGTGGCCG-3′ (NeuroD1), respectively. Then, the PCR products were inserted into Mlu I to Xho I (for Ascl1) and Kpn I to BglII (for NeuroD1) sites of pGL_3 basic vector (Promega). For expression of PCP4/PEP19 in *E. coli*, the coding region of PCP4/PEP19 was generated from the vector including PCP4/PEP19 open reading frame cDNA (GeneCopoeia, Rockville, MD, USA) using PCR, and was inserted into BamHI and SalI sites of pCold TF vector (TF-tagged PCP4/PEP19 expression, Takara Bio, Shiga, Japan) and pGEX-6P vector (GST-tagged PCP4/PEP19 expression, GE Healthcare).

Luciferase reporter assays

M17 cells were seeded at a density of 1×10^4 cells/well in 96-well plates, and 100 ng of reporter plasmid and 5 ng of Renilla luciferase control vector pRL-TK (TOYO B-Net, Tokyo, Japan) were transfected by Lipofectamine 3000 (Thermo Fisher Scientific). On the next day, cells were lysed and the luciferase activities were measured using PicaGene Dual Reagent (TOYO B-Net). The luciferase bioluminescence was quantified using PHELIOS luminometer (Atto, Tokyo, Japan) and the values were normalized by luminescence of Renilla luciferase.

Western blot analysis

M17 cells were precipitated with 10% trichloroacetic acid on ice for 30 min. The precipitates were washed with cold PBS and dissolved in cold lysis buffer (50 mM Tris-HCl [pH 6.8], 2% SDS, 10% glycerol, 6% 2-mercaptoethanol and 0.01% bromophenol blue). The lysates (1 μg/lane) were loaded on precast polyacrylamide gels (10% Bis-Tris Plus Gels, Thermo Fisher Scientific), and transferred to PVDF membranes. The membranes were blocked using 5% nonfat dried milk in TBS (pH 7.6) with 0.1% Tween 20 for 1 h and incubated overnight at 4 °C with primary antibody diluted in Can Get Signal solution 1 (Toyobo) and with a horseradish peroxidase conjugated goat anti-guinea pig antibody (Jackson ImmunoResearch, West Grove, PA, USA) or goat anti-rabbit or mouse antibody (Cell Signaling Technology, Danvers, MA, USA) for 1 h at RT. Anti-PCP4/PEP19 polyclonal guinea pig in-house custom-made antibody was used at 0.2 μg/mL. Anti-PCP4/PEP19 commercial antibody was purchased from Sigma-Aldrich, and was used at 1:250. Antibodies against glyceraldehyde-3-phosphate dehydrogenase (GAPDH), histone deacetylase 1 (HDAC1), MEK1 (clone: 61B12), and NeuroD1 (clone: D35G2) were purchased from Cell Signaling Technology (Danvers, MA, USA). Anti-Ascl1 (MASH1, clone: 24B72D11.1) antibody was purchased from Becton, Dickinson and Company (Franklin Lakes, NJ, USA). These antibodies were used at 1:1000 or 1:2000 concentration. The target proteins were detected with SuperSignal West Pico Chemiluminescent Substrate or SuperSignal West Femto Maximum Sensitivity Substrate (Thermo Fisher Scientific). Densitometry was imaged using Ez-Capture MG (Atto) and analyzed by CS Analyzer 3.0 software (Atto). For antibody absorption test, anti-PCP4/PEP19 in-house custom-made antibody was mixed with TF-tagged PCP4/PEP19 (1:20 molar ratio), and was incubated overnight at 4 °C. The antibody specificity was also tested by immunohistochemistry using formalin-fixed paraffin-embedded human cerebellum tissue sections. For subcellular fractionation of PCP4/PEP19 expression, the cell lysates were fractioned into cytoplasmic and nuclear fractions using a commercial kit (NE-PER nuclear and cytoplasmic extraction reagents, Thermo Scientific) and applied to western blotting.

Immunohistochemistry of human neuroblastoma tissues

Twenty-one cases of surgically resected human neuroblastoma, ganglioneuroblastoma, and ganglioneuroma tissues were collected at Kagoshima University Hospital from 2017 to 2019. The tissues were fixed with buffered neutral 10% formalin, embedded in paraffin blocks, and processed for routine hematoxylin and eosin staining, followed by pathological diagnosis by board-certified pathologists according to WHO classification [21]. Representative tissue sections were used for the immunohistochemical (IHC) studies for the detection of PCP4/PEP19 expression using in-house custom-made anti-PCP4/PEP19 antibody described above. Intense IHC reaction in more than 1% of tumor cells was defined as positive for PCP4/PEP19 expression.

Statistics

All experiments were performed at least three to six times independently and all the data are presented as mean ± SE. Statistical significance was determined by unpaired one-tailed Student's t test and chi-square test, and $p < 0.05$ was considered as statistically significant.

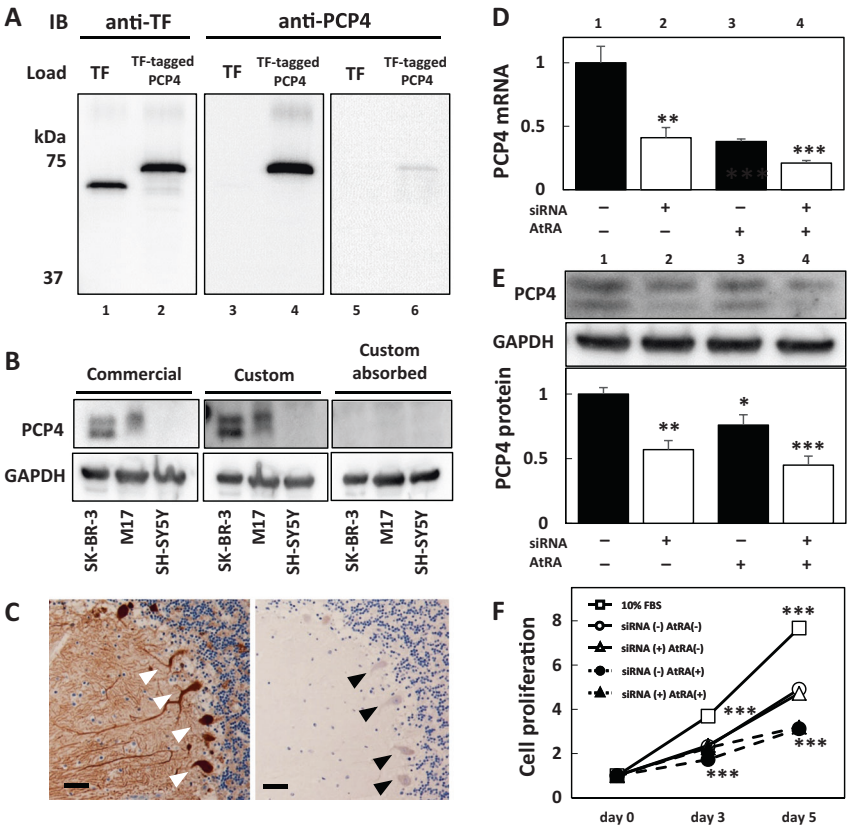

Fig. 1 Anti-PCP4/PEP19 antibody preparation, and effects of AtRA and siRNA effects on PCP4/PEP19 expression and proliferation of M17 cells. Western blotting and immunohistochemistry to show the antibody specificity for PCP4/PEP19. Total lysates of *E. coli* transfected with TF-tagged control and TF-tagged PCP4/PEP19 vectors were analyzed. **a** Anti-TF antibody detected the TF tag protein (Lane 1) and TF-tagged PCP4/PEP19 protein (Lane 2). The same membrane was reprobed with anti-PCP4/PEP19 antibody and only TF-tagged PCP4/PEP19 was recognized (Lane 4). The reactivity of anti-PCP4/PEP19 antibody was reduced after absorption with the recombinant TF-tagged PCP4/PEP19 protein (Lane 6). **b** Cell lysates extracted from SK-BR-3 (positive control), SH-SY5Y (negative control), and M17 cells were subjected to western blotting using custom-made and commercially available antibodies. Both antibodies detected PCP4/PEP19 in SK-BR-3 and M17 lysates but not in the SH-SY5Y lysate, and the reaction disappeared after absorption test. **c** Immunohistochemistry demonstrating PCP4/PEP19 localization in rat cerebellum. The antibody (left panel), but not the absorbed antibody (right panel), detected the Purkinje cell cytoplasm and neurites (arrow heads, original magnification × 200). Expression of PCP4/PEP19 mRNA and protein in M17 cells was monitored by qRT-PCR and western blotting. **d** PCP4/PEP19 mRNA expression was reduced by siRNA (Lanes 2 and 4) and AtRA administration (Lanes 3 and 4) as compared with control (Lane 1). $^{**}p < 0.01$; $^{***}p < 0.001$ vs. control (Lane 1). **e** Same profile was noted for PCP4/PEP19 protein expression. The basal expression (Lane 1) decreased after siRNA transfection (Lanes 2 and 4). Equal protein loading for SDS-PAGE and western blotting was demonstrated by equal detection of GAPDH as an internal control. $^{*}p < 0.05$; $^{**}p < 0.01$; $^{***}p < 0.001$ vs. control (Lane 1). **f** For the siRNA experiments, culturing in 2% FBS-containing medium, the cell growth rate was reduced compared with that observed in 10% FBS-containing medium (open square), but it did not change in the presence and absence of PCP4/PEP19 knockdown (open triangle and open circle, respectively. With AtRA treatment, cell growth rate was decreased in the presence and absence of PCP4/PEP19 knockdown (closed triangle and closed circle, respectively). $^{***}p < 0.001$ vs. control siRNA/2% FBS (open circle).

Results

Preparation of a specific anti-human PCP4/PEP19 antibody

The specificity of the guinea pig polyclonal anti-human PCP4/PEP19 antibody was determined by western blotting. The antibody specifically detected the TF-tagged PCP4/PEP19 protein expressed in *E. coli* (Lane 4, Fig. 1a), which was also recognized by anti-TF antibody (Lane 2, Fig. 1a), and its reactivity was markedly reduced after the antibody was preabsorbed with the recombinant TF-tagged PCP4/PEP19 protein (Lane 6, Fig. 1a). As the protein modification of PCP4/PEP19 would not occur in *E. coli*, the antibody only detected a single band. In contrast, in case of mammalian M17 and SK-BR3 cells, in which a protein modification such as phosphorylation or glycosylation would occur, showed two bands of PCP4/PEP19 detected by the custom-made as well as commercially available antibodies. Another human neuroblastoma cell line

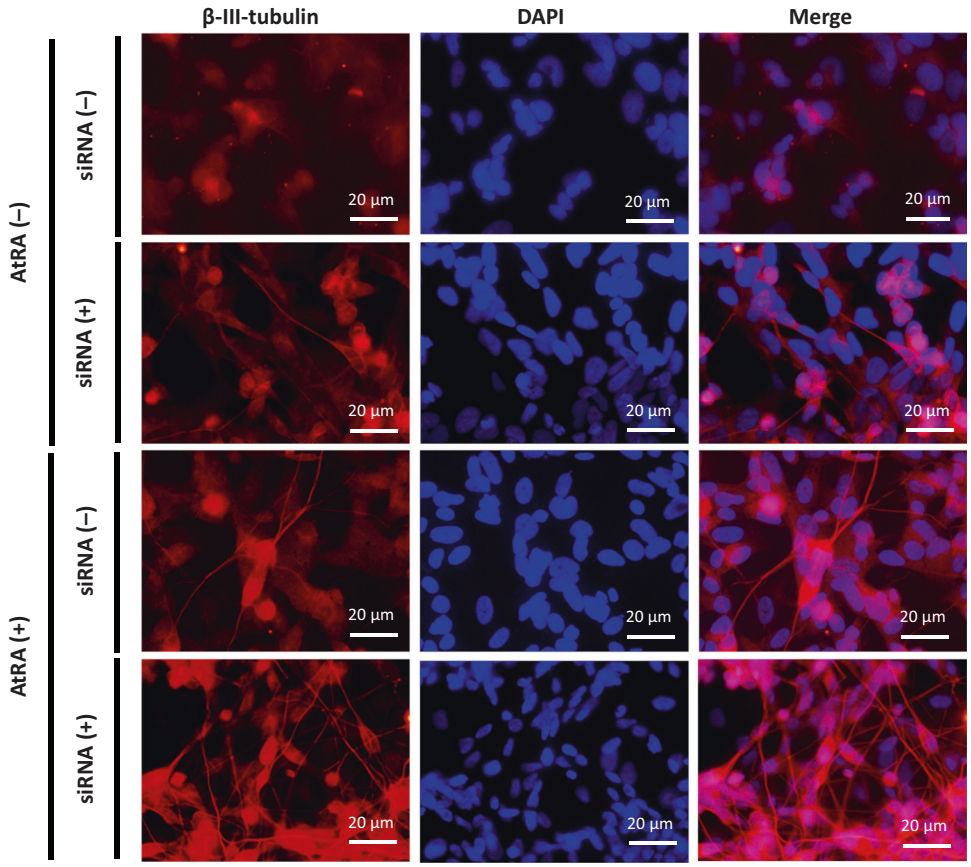

Fig. 2 Neurite outgrowth and neuronal differentiation after AtRA treatment and PCP4/PEP19 knockdown monitored by tubulin immunostaining. The morphological demonstration of neurite outgrowth in cultured M17 cells treated with AtRA and PCP4/PEP19 siRNA. Without AtRA treatment and PCP4/PEP19 knockdown, M17 cells display round to oval shape without dendritic cytoplasmic protrusion. After PCP4/PEP19 siRNA treatment, neurite outgrowth was indicated by red fluorescence for β-III tubulin localization. Similar morphological changes were observed in the cells treated with AtRT. Both PCP4/PEP19 knockdown and AtRA treatment further increased the neurite outgrowth. β-III tubulin, red; nuclei, blue (DAPI).

SH-SY5Y cells did not express PCP4/PEP19. The absorption test abolished the reactivities for the detection of PCP4/PEP19 (Fig. 1b). As shown in Fig. 1c, the antibody also specifically detected the Purkinje cells in human cerebellum by immunohistochemistry (left panel), while the absorbed antibody did not (right panel).

Effect of AtRA on PCP4/PEP19 expression and PCP4/PEP19 knockdown in M17 cells

Human neuroblastoma M17 cells constitutively expressed PCP4/PEP19 mRNA and protein (Lane 1, Fig. 1d, e). AtRA treatment reduced PCP4/PEP19 expression at both the mRNA and protein levels (Lanes 3 and 4, Fig. 1d, e). Knockdown of PCP4/PEP19 by siRNA transfection decreased the protein expression in the presence and absence of AtRA treatment (Lanes 2 and 3, Fig. 1d, e). As AtRA induces neuronal differentiation, these data suggest that PCP4/PEP19 knockdown may also induce neuronal differentiation or that PCP4/PEP19 downregulates neuronal differentiation.

PCP4/PEP19 knockdown does not induce apoptosis in M17 cells

M17 cells increased in numbers during 5 day culture in 10% FBS-containing medium, which is normally for cell expansion and maintenance, (open square, Fig. 1f). For the siRNA experiments, the cells were cultured in 2% FBS-containing medium. In this culture condition, the cell growth rate was reduced compared with that observed in 10% FBS-containing medium, but it did not change in the presence and absence of PCP4/PEP19 knockdown (open triangle and open circle, respectively, Fig. 1f). When the cells were treated with AtRA, cell growth rate was decreased in the presence and absence of PCP4/PEP19 knockdown (closed triangle and closed circle, respectively, Fig. 1f). This indicates that decreased PCP4/PEP19 expression could not induce apoptosis in M17 cells, unlike breast cancer cells as previously reported [8].

PCP4/PEP19 knockdown affects neurite elongation but not number of neurites per cell

The morphological changes and neurite outgrowth in cultured M17 cells treated with AtRA and PCP4/PEP19 siRNA were investigated by β-III tubulin immunofluorescence and fluorescent phalloidin staining. With β-III tubulin immunostaining, without AtRA treatment and PCP4/PEP19 knockdown, M17 cells showed poorly differentiation, round to oval cell morphology, and had no dendritic cytoplasmic protrusion. When the cells were exposed to AtRA or transfected with PCP4/PEP19 siRNA, neurite outgrowth,

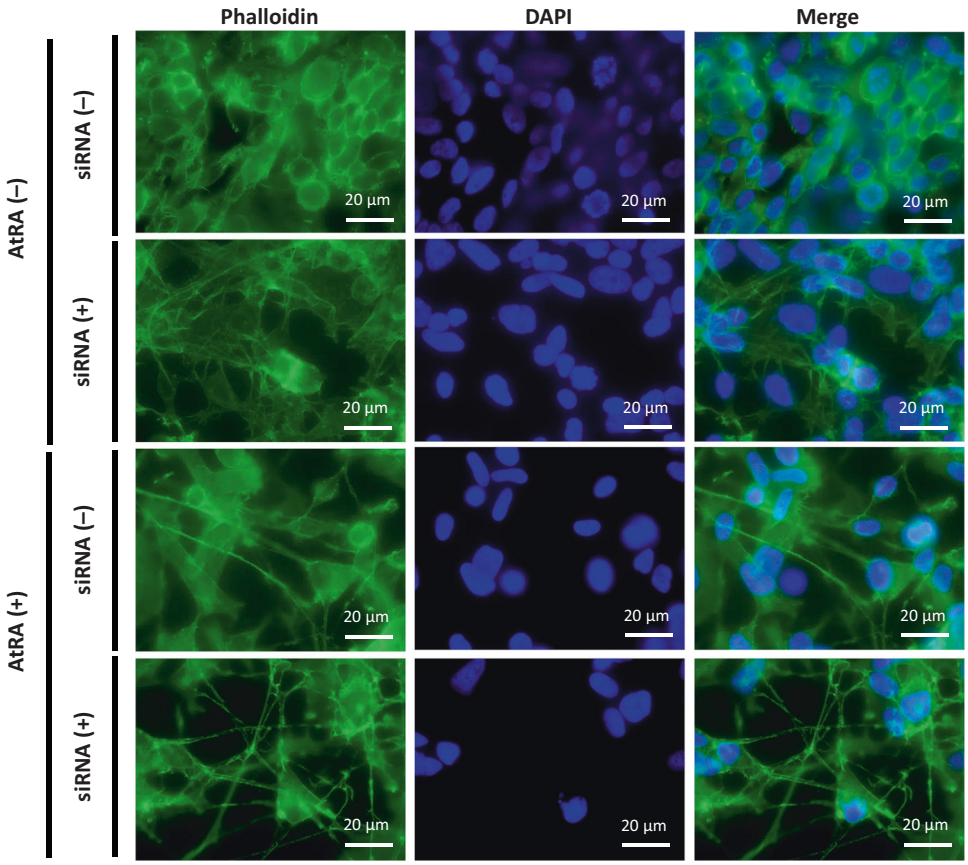

Fig. 3 Neurite outgrowth and neuronal differentiation after AtRA treatment and PCP4/PEP19 knockdown monitored by actin distribution. The morphological demonstration of neurite outgrowth in M17 cells treated with AtRA and PCP4/PEP19 siRNA. Similar morphological changes in neurite outgrowth were observed with phalloidin staining. Actin, green (phalloidin); nuclei, blue (DAPI).

monitored by β-III tubulin localization, was markedly induced (Fig. 2). Similar morphological changes were observed by phalloidin staining, demonstrating actin distribution and neurite outgrowth (Fig. 3).

The phase-contrast photomicrographs also demonstrated neurite outgrowth by AtRA treatment and PCP4/PEP19 knockdown (Fig. 4a). Morphometric analysis showed that the length of neurites increased upon AtRA treatment and PCP4/PEP19 knockdown, which indicates an additive effect on the neurite elongation (Fig. 4b). The neurite counts per cell increased in number upon AtRA treatment, but not upon PCP4/PEP19 knockdown (Fig. 4c). Increase of % cells with neurites was also observed only in AtRA-treated but not in PCP4/PEP19-knocked down cells (Fig. 4d), suggesting that PCP4/PEP19 essentially suppresses the preexisting neurite elongation but not the neurite budding.

Effect of PCP4/PEP19 knockdown on neuronal differentiation factors

To explore the mechanism(s) underlying the regulation of neurite outgrowth by PCP4/PEP19, protein and mRNA expression of neuronal differentiation factors was measured using western blotting and qRT-PCR (the primers are listed in Table 1), respectively. Among these, only Ascl1 and NeuroD1 were regulated by PCP4/PEP19. Ascl1 expression was downregulated by PCP4/PEP19 knockdown but upregulated by the AtRA treatment. The increased expression of Ascl1 by AtRA stimulation was attenuated by PCP4/PEP19 knockdown (Fig. 5a). Conversely, NeuroD1 expression increased after PCP4/PEP19 knockdown. Stimulation with AtRA markedly reduced the NeuroD1 expression but PCP4/PEP19 knockdown recovered it (Fig. 5b). Expression of Map2, Tubb3, Hes1, ID1, ID3, and Ets1 mRNA was increased, while that of vimentin and Notch1 mRNA was reduced by AtRT treatment (data not shown).

PCP4/PEP19 regulates expression of Ascl1 and NeuroD1 at the transcriptional level

To investigate the transcriptional regulation of Ascl1 and NeuroD1 expression by PCP4/PEP19, luciferase reporter assay using Ascl1 and NeuroD1 promoter regions were performed in M17 cells (Fig. 5c). The transcriptional activity of Ascl1 promoter decreased upon PCP4/PEP19 knockdown but increased with AtRA treatment, in which case the increased activity was decreased again upon the PCP4/PEP19 knockdown. Instead, the transcriptional activity of NeuroD1 promoter was clearly enhanced by PCP4/PEP19 knockdown but reduced by AtRA, in which

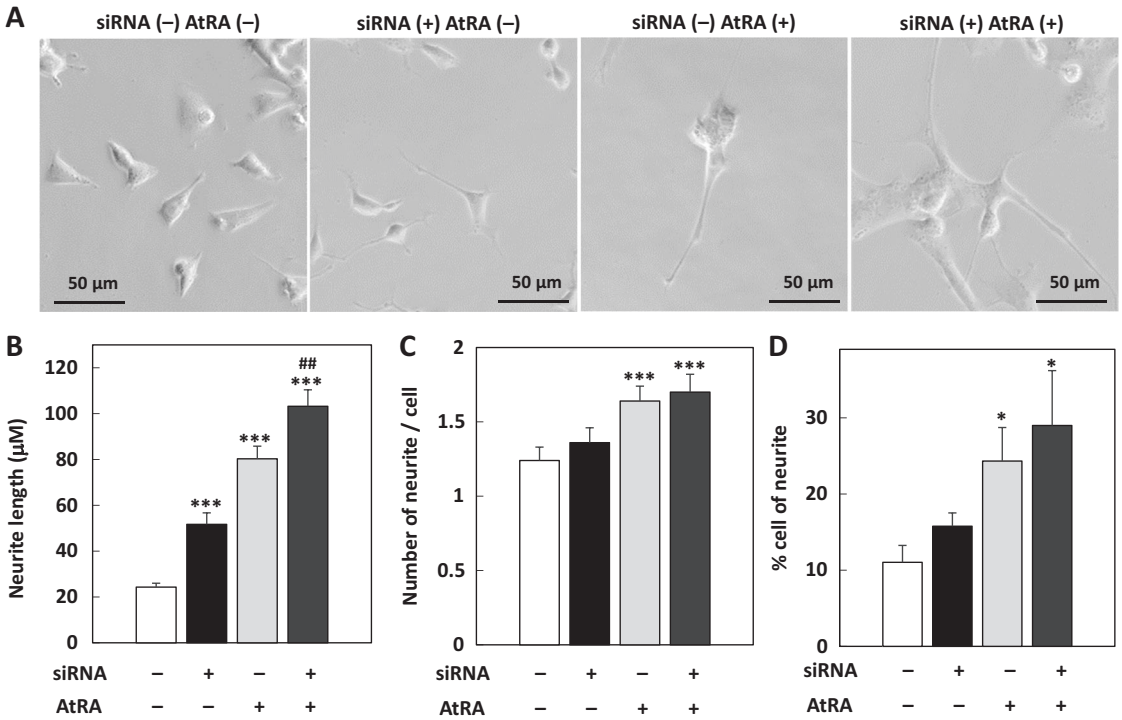

Fig. 4 Morphometric analysis of neurite outgrowth. The degree of neurite outgrowth was analyzed by morphometry from the immunofluorescence images of β-III tubulin. **a** The phase-contrast photomicrographs also demonstrated neurite outgrowth by AtRA treatment and PCP4/PEP19 knockdown. **b** Neurite outgrowth increased upon AtRA treatment as well as PCP4/PEP19 knockdown. Both AtRA treatment and PCP4/PEP19 knockdown demonstrated an additive effect on neurite elongation. **c** Neurite numbers per cell increased upon AtRA treatment, but not upon PCP4/PEP19 knockdown. **d** Percentage increase of cells with neurites was observed in AtRA-treated cells but not in PCP4/PEP19 knockdown cells. $^{*}p < 0.05$ and $^{***}p < 0.001$ vs. siRNA(−)/AtRA(−) control; $^{\#\#}p < 0.01$ between siRNA(−)/AtRA(+) and siRNA(+)/AtRA(+).

case the decreased activity was partially improved by PCP4/PEP19 knockdown.

Effect of Ascl1 and NeuroD1 knockdown on PCP4/PEP19 expression

Next, the effect of Ascl1 and NeuroD1 on PCP4/PEP19 expression was studied using qRT-PCR (Fig. 6a). After Ascl1 knockdown, PCP4/PEP19 was downregulated (column 8) and NeuroD1 was upregulated (column 5) at the mRNA level. When NeuroD1 expression was reduced by siRNA, however, Ascl1 and PCP4/PEP19 mRNA expression levels did not change (columns 3 and 9), indicating that NeuroD1 may be involved in the downstream signaling of Ascl1 and PCP4/PEP19.

Effect of PCP4/PEP19 overexpression on Ascl1 and NeuroD1 expression in SH-SY5Y cells

When the PCP4/PEP19-deficient SH-SY5Y cells (see Fig. 1b) were treated with AtRA, Ascl1 and NeuroD1 mRNA expression significantly decreased (Fig. 6b). With the transfection of PCP4/PEP19 expressing plasmid, Ascl1 and NeuroD1 mRNA expression did not change in the presence and absence of AtRA treatment.

Subcellular localization of PCP4/PEP19 in M17 cells and human neuroblastoma tissues

Clinical information and IHC results are summarized in Table 2. Most of the neuroblastomas, ganglioneuroblastomas, and ganglioneuromas were positive for PCP4/PEP19 (18/21 cases), among which the % positive areas varied from 1 to 90% (average area 20%). PCP4/PEP19 was mostly located in the nuclei of the undifferentiated blastic cells (Fig. 7a–d) and was, by contrast, located in the cytoplasm of mature ganglion cells (Fig. 7e, f). However, the frequency of nuclear and cytoplasmic localization was not significantly different between blastic and non-blastic cells in the PCP4/PEP19-positive 18 cases (Fig. 7g). The degree of expression and subcellular distribution of PCP4/PEP19 were not correlated to the pathological grading and clinical outcome of neuroblastoma cases (data not shown). In M17 cells, PCP4/PEP19 expression was detected in both cytoplasmic and nuclear fractions by western blotting (Fig. 7h).

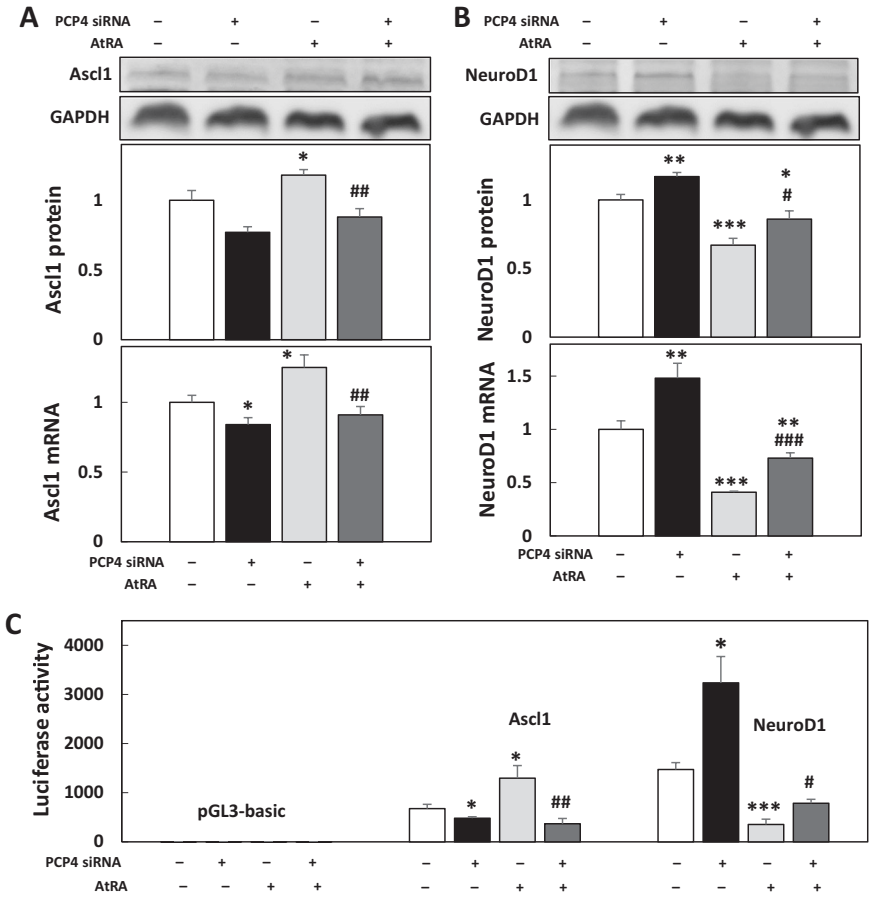

Fig. 5 Effects of PCP4/PEP19 and AtRA on Ascl1 and NeuroD1 expression. Protein and mRNA expression of Ascl1 and NeuroD1 was regulated by PCP4/PEP19 at the transcriptional levels. **a** Ascl1 protein and mRNA expression was decreased by PCP4/PEP19 knockdown but increased by AtRA treatment. The increased expression of Ascl1 by AtRA stimulation was diminished by PCP4/PEP19 knockdown. **b** NeuroD1 protein and mRNA expression increased after PCP4/PEP19 knockdown. AtRA treatment reduced NeuroD1 expression but PCP4/PEP19 knockdown recovered it. **c** Luciferase reporter assay using Ascl1 and NeuroD1 promoter regions after AtRA treatment and PCP4/PEP19 knockdown. Ascl1 promoter activities were reduced by PCP4/PEP19 knockdown but increased by AtRA, in which case the activities were reduced again by PCP4/PEP19 knockdown. The transcriptional activities of NeuroD1 promoter were enhanced by PCP4/PEP19 knockdown but reduced by AtRA, in which case the decreased activities were improved by PCP4/PEP19 knockdown. The pGL_3 basic vector was used as a control for luciferase assay. $^{*}p < 0.05$, $^{**}p < 0.01$, and $^{***}p < 0.001$ vs. siRNA(−)/AtRA(−) control; $^{\#}p < 0.05$, $^{\#\#}p < 0.01$, and $^{\#\#\#}p < 0.001$ between siRNA(−)/AtRA(+) and siRNA(+)/AtRA(+).

Discussion

In the present study, we investigated the effects of PCP4/PEP19 on neural cell morphology and neurite outgrowth, which is one of the essential events for neural cells, using human neuroblastoma M17 cells. Our experiments suggest that PCP4/PEP19 suppresses neurite outgrowth of M17 cells through transcriptional regulation of Ascl1 and NeuroD1 expression. The proposed model of PCP4/PEP19 regulation in neuronal differentiation is presented in a schema (Fig. 8).

PCP4/PEP19 was originally reported as an antiapoptotic factor for neuronal cells [14] and our previous studies also demonstrated an inhibitory effect of PCP4/PEP19 on cancer cell apoptosis and a promoting effect on migration and invasion [8, 11, 12]. However, only one report had shown that PCP4/PEP19 could be a differentiation factor for rat pheochromocytoma-derived PC12 paraneuronal cells, promoting the neuroendocrine differentiation and neurite outgrowth [13].

M17 cells are derived from human adrenal neuroblastoma and have a poorly differentiated cellular morphology with no neurite growth in usual culture conditions [22]. By stimulating with AtRA and 12-O-tetradecanoylphorbol-13-acetate (TPA), M17 cells acquire differentiated features, which include elongated cell shape and extensive neurite outgrowth. In addition to the morphological changes in cell culture, AtRA and TPA treatment were found to induce the expression of some differentiation markers, such as β-III tubulin, MAP2, synaptophysin, and

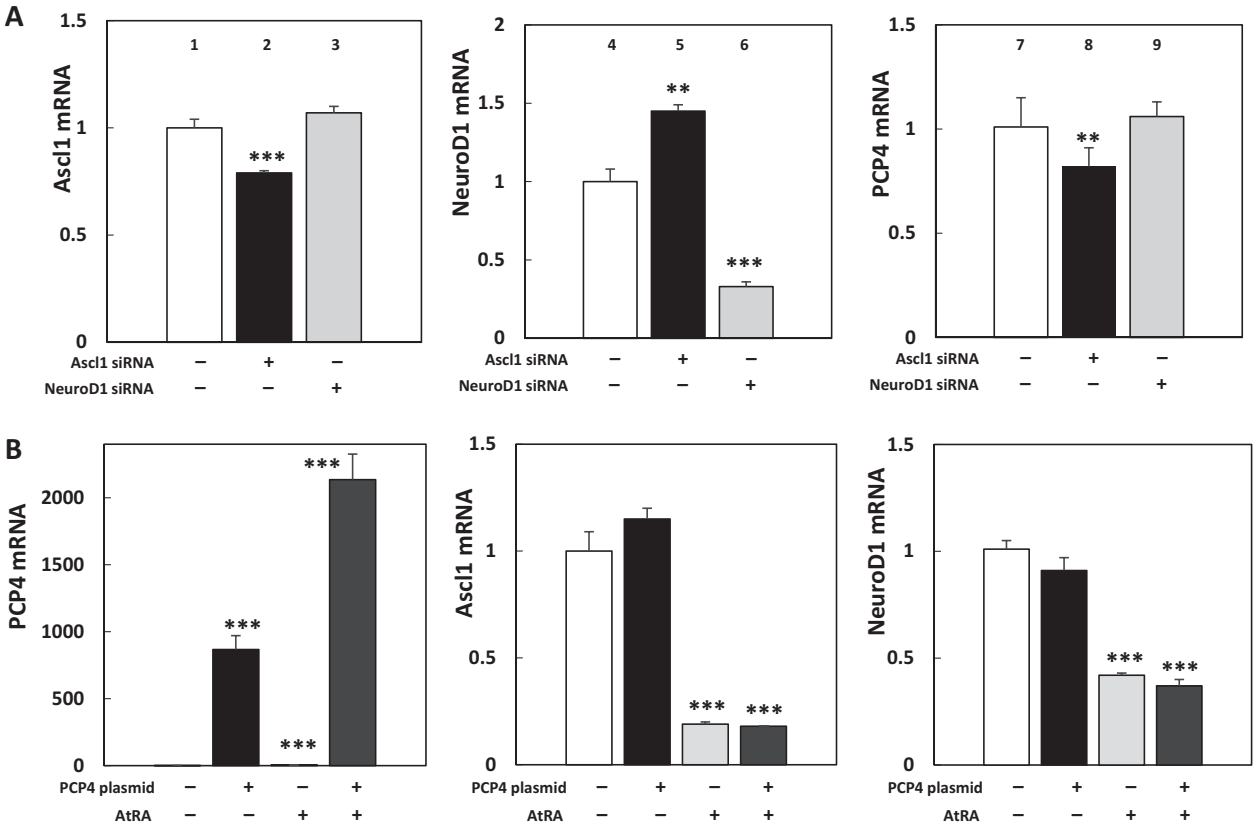

Fig. 6 Relation of PCP4/PEP19, Ascl1, and NeuroD1 expression in M17 and SH-SY5Y cells. a Effects of Ascl1 and NeuroD1 on PCP4/PEP19 expression were studied by qRT-PCR. After Ascl1 knockdown, mRNA expression of PCP4/PEP19 decreased (column 8) and that of NeuroD1 increased (column 5). NeuroD1 knockdown did not change either Ascl1 or PCP4/PEP19 mRNA expression levels (columns 3 and 9). **b** Ascl1 and NeuroD1 mRNA expression significantly decreased in the SH-SY5Y cells after AtRA treatment. After PCP4/PEP19 overexpression, Ascl1 and NeuroD1 mRNA expression did not change in the presence and absence of AtRA treatment. $^{**}p < 0.01$, and $^{***}p < 0.001$ vs. both siRNA negative control.

nestin [23]. Exogenous overexpression of miR-124 using lentivirus vector also induces neuronal differentiation in M17 cells, and enhances the catecholaminergic differentiation [24]. During M17 differentiation into mature neuronal cells, many differentiation markers are expressed sequentially, depending on the maturation status. In the present study, increased neurite elongation and expression of β-III tubulin and NeuroD1 were consistently observed after AtRA stimulation and PCP4/PEP19 knockdown in M17 cells. SH-SY5Y is another undifferentiated human neuroblastoma cell line also used in studies of neuronal differentiation [23]. SH-SY5Y cells, however, did not express PCP4/PEP19 in our experimental conditions, and the expression of Ascl1 and NeuroD1 did not change even after PCP4/PEP19 overexpression. Conversely, in PCP4/PEP19-positive PC12 cells, which are originated from rat pheochromocytoma of the adrenal medulla, PCP4/PEP19 enhances neurite outgrowth and neuroendocrine differentiation [13]. Therefore, PCP4/PEP19 can differentially regulate the neuronal or neuroendocrine differentiation between paraneuron-like PC12 cells, immature neuron-like M17, and SH-SY5Y cells. Although PCP4/PEP19 gene-modified mice, both knockout and transgenic, show phenotypes with impairment in higher brain functions, and neural PCP4/PEP19 expression decreases in Alzheimer's and Huntington's disease and with alcoholism [5, 6], the role of PCP4/PEP19 in neuronal differentiation and functions are still highly controversial.

AtRA treatment and PCP4/PEP19 knockdown resulted in the contradictory change in Ascl1 and NeuroD1 expression in M17 cells. Both Ascl1 and NeuroD1 are transcription factors that function as lineage-specific neuronal differentiation markers. Ascl1 is expressed at the stages of neural stem cells to intermediate progenitors, while NeuroD1 at more mature stages of intermediate progenitors to immature neurons [25–27]. Therefore, AtRA might stimulate the neural stem cells to differentiate into intermediate progenitor cells via upregulation of Ascl1 and downregulation of NeuroD1 in human neuroblastoma M17 cells. In contrast, PCP4/PEP19 knockdown counteracted the AtRA effects on the expression of Ascl1 and NeuroD1, indicating that normally expressed PCP4/PEP19 could

Table 2 Clinical, histological, and immunohistochemical summaries.

				Histological diagnosis		PCP4/PEP19 IHC	
No.	Sex	Age	Anatomic site	Classification	Cell types	Nuclear localization	Positive % area
1	M	4	Retroperitoneum	Neuroblastoma, poorly differentiated	G−, D+, B+	(−)	0
2	M	3	Left kidney	Neuroblastoma, NOS	G+, D+, B−	(−)	30
3	F	3	Retroperitoneum	Neuroblastoma, poorly differentiated	G−, D−, B+	(+)	1
4	F	2	Neck	Neuroblastoma, poorly differentiated	G−, D−, B+	(−)	0
5	M	4	Right adrenal gland	Ganglioneuroblastoma, intermixed	G+, D+, B−	(+)	10
6	M	4	Adrenal gland	Neuroblastoma, poorly differentiated	G−, D−, B+	(+)	10
7	M	2	Left adrenal gland	Neuroblastoma, NOS	G+, D+, B+	(+)	10
8	F	58	Mediastinum	Ganglioneuroblastoma, intermixed	G+, D+, B−	(−)	50
9	M	30	Right adrenal gland	Ganglioneuroma, mature	G+, D−, B−	(−)	40
10	M	67	Left adrenal gland	Ganglioneuroma, NOS	G+, D−, B−	(−)	30
11	M	1	Right adrenal gland	Neuroblastoma, poorly differentiated	G−, D−, B+	(−)	0
12	M	0	Pelvic cavity	Neuroblastoma, poorly differentiated,	G−, D−, B+	(+)	30
13	M	8	Retroperitoneum	Neuroblastoma, poorly differentiated	G−, D−, B+	(−)	10
14	M	7	Right adrenal gland	Neuroblastoma, poorly differentiated	G−, D−, B+	(+)	1
15	M	8	Retroperitoneum	Ganglioneuroblastoma, nodular	G−, D+, B+	(−)	40
16	F	3	Left adrenal gland	Neuroblastoma, poorly differentiated	G−, D+, B+	(−)	90
17	F	1	Right adrenal gland	Neuroblastoma, poorly differentiated	G−, D−, B+	(+)	1
18	F	3	Right adrenal gland	Neuroblastoma, poorly differentiated	G−, D+, B+	(−)	1
19	F	1	Left adrenal gland	Neuroblastoma, poorly differentiated	G−, D−, B+	(+)	10
20	M	0	Right adrenal gland	Neuroblastoma, poorly differentiated	G−, D+, B+	(−)	20
21	M	7	Left adrenal gland	Neuroblastoma, poorly differentiated	G−, D+, B+	(+)	20

G ganglion cells, *D* differentiating cells, *B* blastic cells.

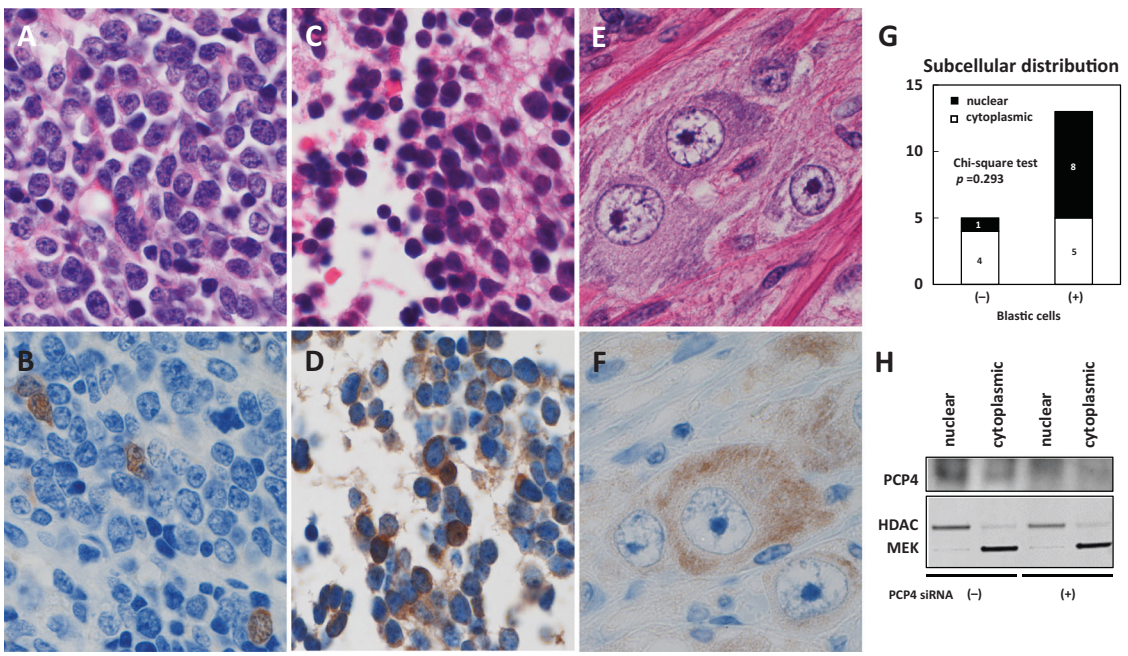

Fig. 7 Subcellular localization of PCP4/PEP19 in human neuroblastoma tissues and M17 cells. Representative photomicrographs of PCP4/PEP19 immunohistochemistry are shown. Most of the undifferentiated blastic cells in neuroblastoma (case no. 6 and no. 12) (**a**, **c**, **h**, **e**) were positive for nuclear PCP4/PEP19 expression (**b**, **d**, IHC). Some blastic cells showed cytoplasmic PCP4/PEP19 localization (**d**). By contrast, mature ganglion-like cells (case no. 2) (**e**, **h**, **e**) were positive for cytoplasmic PCP4/PEP19 expression (**f**, IHC). (Original magnification × 400.) **g** The frequency of nuclear and cytoplasmic expression was not significantly different between blastic and non-blastic cells in PCP4/PEP19-positive 18 cases. **h** PCP4/PEP19 expression was detected in both cytoplasmic and nuclear fractions by western blotting. HDAC1 and MEK1 expression was monitored as positive control for nuclear and cytoplasmic expression, respectively.

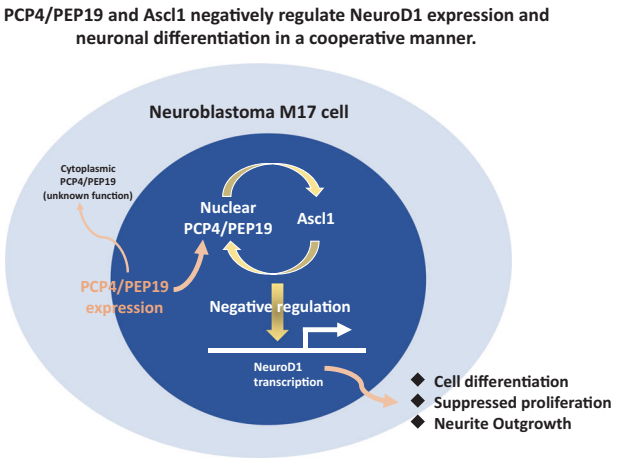

Fig. 8 Schematic presentation of PCP4/PEP19 regulation of neural differentiation in neuroblastoma M17 cells. A possible mechanism of neural differentiation of M17 cells by PCP4/PEP19 mediate through NeuroD1 and Ascl1 expression was shown. PCP4/PEP19 and Ascl1 would negatively regulate the NeuroD1 expression and neuronal differentiation in a cooperative manner.

cooperate with AtRA on the regulation of Ascl1 and NeuroD1 expression but suppress the neuronal differentiation and neurite outgrowth. Further studies focused on the stage specific knockdown of PCP4/PEP19, Asc11 and NeuroD1 in neural stem or progenitor cells with AtRA treatment are necessary to clarify the interaction between AtRA and PCP4/PEP19 on Ascl1 and NeuroD1 expression.

We showed that Ascl1 and PCP4/PEP19 regulate each other, whereby knockdown of one decreased the expression of the other, and that PCP4/PEP19 and Ascl1 knockdown separately increased NeuroD1 expression. NeuroD1 knockdown, however, had no effects on either Ascl1 or PCP4/PEP19 expression. Therefore, PCP4/PEP19 and Ascl1 could be located upstream of NeuroD1 in the signal transduction pathway. In pulmonary small cell carcinoma (a type of neuroendocrine tumor), Ascl1 and NeuroD1 are expressed at higher and lower levels to regulate neuroendocrine and neuronal gene expression, respectively, but only the Ascl1 directly upregulates the oncogene expression [28]. Although we do not know whether the PCP4/PEP19, Ascl1, and NeuroD1 might play any important roles in carcinogenesis, such as oncogenes, in neuroblastoma M17 cells; PCP4/PEP19 and Ascl1 negatively regulated the NeuroD1 expression and neuronal differentiation in a cooperative manner.

By IHC analysis of clinical specimens, we clearly demonstrated that human neuroblastomas express PCP4/PEP19, more frequently in the nuclei of immature blastic cells, indicating that it might function as an intranuclear negative regulator of neuronal differentiation. Taken together with the results obtained from IHC, our study suggests that PCP4/PEP19 could be a potential molecular target for differentiation-induction therapy for neuroblastoma. Differentiation-induction therapy to convert malignant tumor cells into more differentiated and less aggressive cells may be another strategy for cancer treatment in addition to surgical resection, chemotherapy, and radiation [29]. Neuroblastoma is the most common malignant solid tumor in children. It often exhibits heterogeneous differentiation, consisting of poorly differentiated and well differentiated areas [21, 30]. Furthermore, it is well known that the poorly differentiated tumor cells, spontaneously or after chemotherapy, may convert to well differentiated subtypes of ganglioneuroblastoma or ganglioneuroma [31].

The present study has some limitations. First, most experiments were performed using M17 cells, and these cells may not necessarily reflect the characteristics of neuroblastoma in humans. Second, PCP4/PEP19 localizes in both cytoplasm and nuclei of cultured cells and human neuroblastoma tissues, but pathological and clinical significance of the subcellular localization is still unclear. Third, we do not know whether these results can be extrapolated to other types of neuroendocrine tumors, such as small cell lung cancer (SCLC). Given that a new therapeutic strategy is urgently needed to improve the poor prognosis of SCLC; and the expression pattern and function(s) of PCP4/PEP19 in SCLC should be investigated in a future work [32, 33].

Regulation of cell proliferation, apoptosis, mobility, and differentiation determine cancer volumes and malignant potential. In addition to our previous observations that PCP4/PEP19 has regulatory effects on apoptosis and epithelial–mesenchymal transition in human breast cancer cells [8, 11], we demonstrated here a novel function of PCP4/PEP19 as a promoter of cellular differentiation in human neuroblastoma cells. These findings support that PCP4/PEP19 may play pivotal roles in carcinogenesis of certain cancer cell types.

Acknowledgements The authors greatly appreciate the excellent technical assistance of Ms. Orie Iwaya and Ms. Mai Tokudome (Department of Pathology, Kagoshima University Graduate School of Medical and Dental Sciences).

Compliance with ethical standards

Conflict of interest The authors declare that they have no conflict of interest.

Ethics The IHC studies using human tissues were approved by the ethics committees for clinical and epidemiologic research at Kagoshima University.

Publisher's note Springer Nature remains neutral with regard to jurisdictional claims in published maps and institutional affiliations.

References

1. Hockberger PE, Yousif L, Nam SC. Identification of acutely isolated cells from developing rat cerebellum. Neuroimage. 1994;1:276–87.
2. Ziai R, Pan YC, Hulmes JD, Sangameswaran L, Morgan JI. Isolation, sequence, and developmental profile of a brain-specific polypeptide, PEP-19. Proc Natl Acad Sci USA. 1986;83:8420–3.
3. Wei P, Blundon JA, Rong Y, Zakharenko SS, Morgan JI. Impaired locomotor learning and altered cerebellar synaptic plasticity in pep-19/PCP4-null mice. Mol Cell Biol. 2011;31:2838–344.
4. Mouton-Liger F, Thomas S, Rattenbach R, Magnol L, Larigaldie V, Ledru A, et al. PCP4 (PEP19) overexpression induces premature neuronal differentiation associated with Ca(2+)/calmodulin-dependent kinase II-δ activation in mouse models of Down syndrome. J Comp Neurol. 2011;519:2779–802.
5. Utal AK, Stopka AL, Roy M, Coleman PD. PEP-19 immunohistochemistry defines the basal ganglia and associated structures in the adult human brain, and is dramatically reduced in Huntington's disease. Neuroscience. 1998;86:1055–63.
6. Iwamoto K, Bundo M, Yamamoto M, Ozawa H, Saito T, Kato T. Decreased expression of NEFH and PCP4/PEP19 in the prefrontal cortex of alcoholics. Neurosci Res. 2004;49:379–85.
7. Bourdeau V, Deschênes J, Laperrière D, Aid M, White JH, Mader S. Mechanisms of primary and secondary estrogen target gene regulation in breast cancer cells. Nucleic Acids Res. 2008;36:76–93.
8. Hamada T, Souda M, Yoshimura T, Sasaguri S, Hatanaka K, Tasaki T, et al. Anti-apoptotic effects of PCP4/PEP19 in human breast cancer cell lines: a novel oncotarget. Oncotarget. 2014;5:6076–86.
9. Wang T, Satoh F, Morimoto R, Nakamura Y, Sasano H, Auchus RJ, et al. Gene expression profiles in aldosterone-producing adenomas and adjacent adrenal glands. Eur J Endocrinol. 2011;164:613–9.
10. Kanamori T, Takakura K, Mandai M, Kariya M, Fukuhara K, Kusakari T, et al. PEP-19 overexpression in human uterine leiomyoma. Mol Hum Reprod. 2003;9:709–17.
11. Yoshimura T, Hamada T, Hijioka H, Souda M, Hatanaka K, Yoshioka T, et al. PCP4/PEP19 promotes migration, invasion and adhesion in human breast cancer MCF-7 and T47D cells. Oncotarget. 2016;7:49065–74.
12. Honjo K, Hamada T, Yoshimura T, Yokoyama S, Yamada S, Tan YQ, et al. PCP4/PEP19 upregulates aromatase gene expression via CYP19A1 promoter I.1 in human breast cancer SK-BR-3 cells. Oncotarget. 2018;9:29619–33.
13. Harashima S, Wang Y, Horiuchi T, Seino Y, inagaki N. Purkinje cell protein 4 positively regulates neurite outgrowth and neurotransmitter release. J Neurosci Res. 2011;89:1519–30.
14. Erhardt JA, Legos JJ, Johanson RA, Slemmon JR, Wang X. Expression of PEP-19 inhibits apoptosis in PC12 cells. Neuroreport. 2000;11:3719–23.
15. Bowen RL, Verdile G, Liu T, Parlow AF, Perry G, Smith MA, et al. Luteinizing hormone, a reproductive regulator that modulates the processing of amyloid-beta precursor protein and amyloid-beta deposition. J Biol Chem. 2004;279:20539–45.
16. Janesick A, Wu SC, Blumberg B. Retinoic acid signaling and neuronal differentiation. Cell Mol Life Sci. 2015;72:1559–76.
17. Devanna P, Middelbeek J, Vernes SC. FOXP2 drives neuronal differentiation by interacting with retinoic acid signaling pathways. Front Cell Neurosci. 2014;8:305.
18. Oikari LE, Okolicsanyi RK, Griffiths LR, Haupt LM. Data defining markers of human neural stem cell lineage potential. Data Brief. 2016;7:206–15.
19. Hollenhorst PC, Jones DA, Graves BJ. Expression profiles frame the promoter specificity dilemma of the ETS family of transcription factors. Nucleic Acids Res. 2004;32:5693–702.
20. Yoshimatsu Y, Yamazaki T, Mihira H, Itoh T, Suehiro J, Yuki K, et al. Ets family members induce lymphangiogenesis through physical and functional interaction with Prox1. J Cell Sci. 2011;124:2753–62.
21. Shimada H, DeLellis RA, Tissier F. Neuroblastic tumours of the adrenal gland. In: Lloid RV, Osamura RY, Kloppel G, Rosai J, editors. WHO classification of tumours of endocrine organs. 4th ed. Lyon, France: IARC; 2016. p. 196–203.
22. Andres D, Keyser BM, Petrali J, Benton B, Hubbard KS, McNutt PM, et al. Morphological and functional differentiation in BE(2)-M17 human neuroblastoma cells by treatment with trans-retinoic acid. BMC Neurosci. 2013;14:49.
23. Filograna R, Civiero L, Ferrari V, Codolo G, Greggio E, Bubacco L, et al. Analysis of the catecholaminergic phenotype in human SH-SY5Y and BE(2)-M17 neuroblastoma cell lines upon differentiation. PLoS ONE. 2015;10:e0136769.
24. Sharif S, Ghahremani MH, Soleimani M. Induction of morphological and functional differentiation of human neuroblastoma cells by miR-124. J Biosci. 2017;42:555–63.
25. Kim EJ, Ables JL, Dickel LK, Eisch AJ, Johnson JE. Ascl1 (Mash1) defines cells with long-term neurogenic potential in subgranular and subventricular zones in adult mouse brain. PLoS ONE. 2011;6:e18472.
26. Castro DS, Martynoga B, Parras C, Ramesh V, Pacary E, Johnston C, et al. A novel function of the proneural factor Ascl1 in progenitor proliferation identified by genome-wide characterization of its targets. Genes Dev. 2011;25:930–45.
27. von Bohlen und Halbach O. Immunohistological markers for proliferative events, gliogenesis, and neurogenesis within the adult hippocampus. Cell Tissue Res. 2011;345:1–19.
28. Borromeo MD, Savage TK, Kollipara RK, He M, Augustyn A, Osborne JK, et al. ASCL1 and NEUROD1 reveal heterogeneity in pulmonary neuroendocrine tumors and regulate distinct genetic programs. Cell Rep. 2016;16:1259–72.
29. Kawamata H, Tachibana M, Fujimori T, Imai Y. Differentiation-inducing therapy for solid tumors. Curr Pharm Des. 2006;12:379–85.
30. Shimada H, Ambros IM, Dehner LP, Hata J, Joshi VV, Roald B, et al. The International Neuroblastoma Pathology Classification (the Shimada system). Cancer. 1999;86:364–72.
31. Jögi A, Vaapil M, Johansson M, Påhlman S. Cancer cell differentiation heterogeneity and aggressive behavior in solid tumors. Ups J Med Sci. 2012;117:217–24.
32. Bernhardt EB, Jalal SI. Small cell lung cancer. Cancer Treat Res. 2016;170:301–22.
33. Gazdar AF, Bunn PA, Minna JD. Small-cell lung cancer: what we know, what we need to know and the path forward. Nat Rev Cancer. 2017;17:725–37.